JPE 16-2-25

http://dx.doi.org/10.6113/JPE.2016.16.2.654
ISSN(Print): 1598-2092 / ISSN(Online): 2093-4718

A Novel Photovoltaic Power Harvesting System Using a Transformerless H6 Single-Phase Inverter with Improved Grid Current Quality

A. Radhika† and A. Shunmugalatha*

†,*Department of Electrical and Electronics Engineering, Velammal College of Engineering and Technology, Madurai, India

Abstract

The pumping of electric power from photovoltaic (PV) farms is normally carried out using transformers, which require heavy mounting structures and are thus costly, less efficient, and bulky. Therefore, transformerless schemes are developed for the injection of power into the grid. Compared with the H4 inverter topology, the H6 topology is a better choice for pumping PV power into the grid because of the reduced common mode current. This paper presents how the perturb and observe (P&O) algorithm for maximum power point tracking (MPPT) can be implemented in the H6 inverter topology along with the improved sinusoidal current injected to the grid at unity power factor with the average current mode control technique. On the basis of the P&O MPPT algorithm, a power reference for the present insolation level is first calculated. Maintaining this power reference and referring to the AC sine wave of bus bars, a sinusoidal current at unity power factor is injected to the grid. The proportional integral (PI) controller and fuzzy logic controller (FLC) are designed and implemented. The FLC outperforms the PI controller in terms of conversion efficiency and injected power quality. A simulation in the MATLAB/SIMULINK environment is carried out. An experimental prototype is built to validate the proposed idea. The dynamic and steady-state performances of the FLC controller are found to be better than those of the PI controller. The results are presented in this paper.

Key words: Active balancing, Electric vehicle, Rechargeable battery, Switching converter, Transformer

I. INTRODUCTION

With the fast depletion of fossil fuels, the power generation industry is constantly searching for alternative means of power generation via renewable sources [1]. New alternatives focus on the usage of natural resources, such as wind and sunlight, which do not contribute to the problems and threats associated with global warming [2]. Unlike conventional power generators that utilize fossil fuels, modern renewable energy-based power generators cannot offer stable power sourcing because their resources are not naturally available in a steady manner. As such, power conversion systems should be equipped with maximum power point tracking (MPPT), which is a feature that guarantees the maximum possible power generation for the available quantity of solar insolation or wind velocities.

Transformers are bulky and costly, and they consume some power as losses. Thus, developing transformerless power conversion systems is a desirable endeavor. The H6 topology of transformerless inverters derived from H5 and HERIC topologies with a common mode leakage current elimination was proposed in [3]. A high efficiency inverter with an H6-type configuration for photovoltaic (PV) applications was suggested in [4]. A transformerless single-phase multilevel-based PV inverter was proposed in [5], [6].

A single-phase transformerless doubly grounded grid-connected PV interface was developed in [7], [8]. A transformerless split-inductor neutral point clamped three-level PV grid-connected inverter was proposed in [9]. In transformerless power conversion systems, developing the required voltage levels is possible. The leakage of circulating currents that flow through the ground and PV panels is likely. In [10], [11], modulation techniques were demonstrated to

Manuscript received Jun. 13, 2015; accepted Oct. 6, 2015
Recommended for publication by Associate Editor Chun-An Cheng.
†Corresponding Author: aradhika80@gmail.com
Tel: + 91-452-2465289, Velammal College of Engineering and Tech.
*Department of Electrical and Electronics Engineering, Velammal College of Engineering and Technology, India

eliminate leakage currents in transformerless three-phase PV systems. A leakage current analytical model for a transformerless grid-connected PV inverter was presented in [12]. As demonstrated in [13], the H6 inverter scheme adopts a HERIC topology, in which common mode leakage current is minimal. However, this H6 inverter system does not incorporate an MPPT scheme and a strategy to guarantee a sinusoidal source current with a unity power factor.

MPPT techniques for PV applications were discussed in [14]. A literature review of MPPT techniques for PV applications was presented in [15]. A perturb and observe (P&O) MPPT technique was demonstrated in [16]. The adaptive P&O MPPT technique under rapidly changing irradiances was elaborated in [17], [18]. To pump power at a unity power factor, an average current control scheme is generally adopted. An average current mode control scheme for converters was reported in [19], [20]. Therefore, in the present work, the H6 inverter is extended with the addition of a control scheme, which includes the P&O algorithm-based MPPT and the average current control scheme to pump power at a unity power factor with a sinusoidal current. Proportional integral (PI) controllers and fuzzy logic controllers (FLCs) are designed and implemented separately.

The paper is arranged as follows. A brief outline of the H6 inverter scheme is presented in Section II. The implementation of the combined MPPT and the average current controller-based power quality improvement schemes are reported in Section III. A MATLAB/SIMULINK simulation is illustrated in Section IV. The details of the experimental verification are shown in Section V. A discussion on the results is carried out in Section VI. The conclusion and the direction of future research are described in Section VII.

II. A Review Of the H6 Inverter System

The solar panels of PV plants are usually grounded to the earth to avoid electric shock. The grounding of PV panels becomes mandatory in cases of transformerless power injection schemes because of the lack of proper isolation caused by the absence of a transformer. The elimination of the transformer leads to a circulating current between the grid ground and the grounding point of PV panels. The H6 topology overcomes this drawback by providing a circulating path and thus mitigating the leakage current through the ground. In a typical PV farm, a significant parasitic capacitance may exist between the ground of the grid and PV panels. This parasitic capacitance may lead to leakage currents that could further result in electric shock hazards. Hence, problems associated with radiated interferences may emerge.

A number of methodologies have been suggested to reduce leakage current within the limited range of tolerance. In a typical topological arrangement (Figure 2), the leakage current passes through the parasitic capacitances C1 and C2. The other components in the circuit (Figure 2) are the bridge elements, filter elements, grid, and ground impedance. The filter inductances L1 and L2, along with the parasitic capacitance, form a series resonant path. The common mode voltage is given in Equation (1).

The leakage currents can be minimized by maintaining the common mode voltage near a constant value. The half-bridge inverter topology can also help reduce the common mode current. In this case, the center point of the DC link capacitors is tied to the neutral point. This arrangement reduces the overall output voltage. This half-bridge arrangement involves only a single inductor; the common mode voltage is presented in Equation (2). By contrast, a full-bridge arrangement involves two filter inductors of equal values; the common mode voltage is presented in Equation (3).

$$v_{cm} = \frac{v_{AN} + v_{BN}}{2} + (v_{AN} - v_{BN})\frac{2(L_2 - L_1)}{L_1 + L_2} \quad (1)$$

$$v_{cm} = \frac{v_{AN} + v_{BN}}{2} - \frac{(v_{AN} - v_{BN})}{2} = v_{BN} \quad (2)$$

$$v_{cm} = \frac{v_{AN} + v_{BN}}{2} \quad (3)$$

The full-bridge inverter with bipolar sinusoidal pulse width modulation (PWM) is a common technique to deal with common mode voltage. Although its leakage current characteristics are attractive, this method leads to pronounced ripples and thus reduces efficiency. The full-bridge inverter with unipolar sinusoidal PWM reduces ripples, but its common mode voltage, which is a function of switching frequency, is relatively high. Two different approaches have been widely attempted for keeping the common mode voltage constant. In the first approach, the neutral line of the grid is connected to the negative terminal of a PV panel system. In the other method, which is similar to the H6 configuration, the DC and AC sides are disconnected during the freewheeling period. Unlike the normal full-bridge inverter, the second approach involves two additional switches. The AC side or grid side is disconnected from the DC side when the inverter voltage crosses the zero voltage level, thus terminating the leakage current path. The H6 inverter offers minimal switching losses, and it can be slightly altered to bring out a HERIC-type inverter (Figure 4).

The basic H6 inverter shown in Figure 3 can be rearranged, as presented in Figure 4. The switches S5 and S6 help free wheel conduction. The H4 inverter topology is shown in Figure 5.

A switching scheme using a carrier-based sinusoidal PWM is adopted, and six switching pulses are derived from the PWM unit. Figure 6 shows the PWM scheme for generating switching pulses. The current driven into the grid becomes a

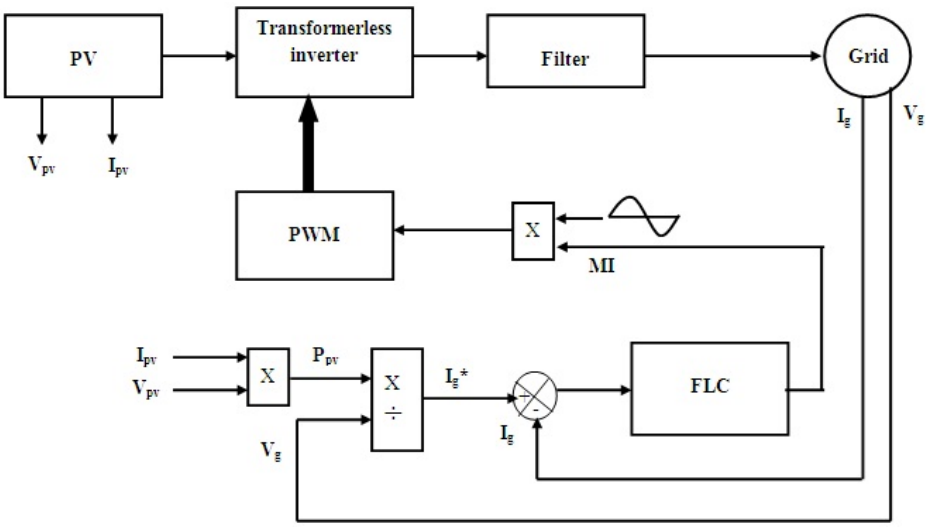

Fig. 1. Block diagram of proposed system.

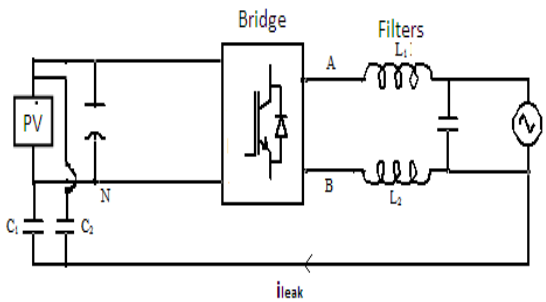

Fig. 2. Transformerless PV inverter.

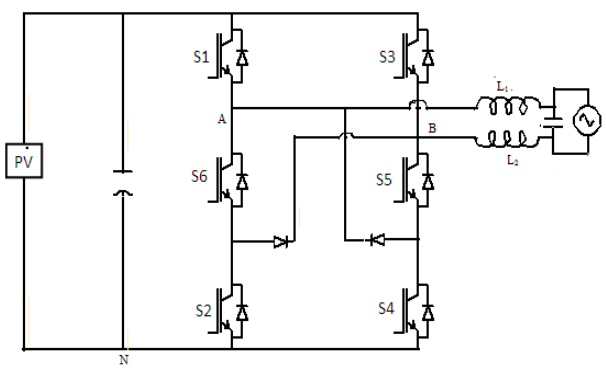

Fig. 3. H6-type transformerless PV inverter.

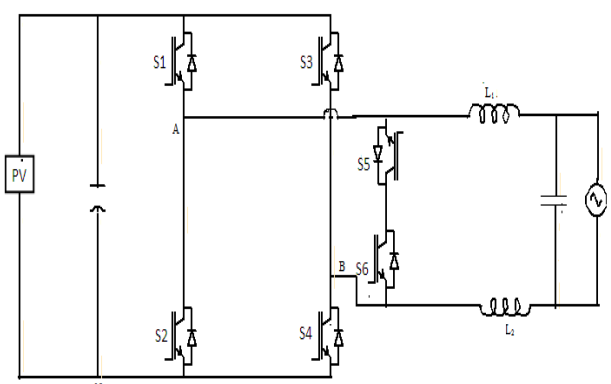

Fig. 4. HERIC-type transformerless PV inverter.

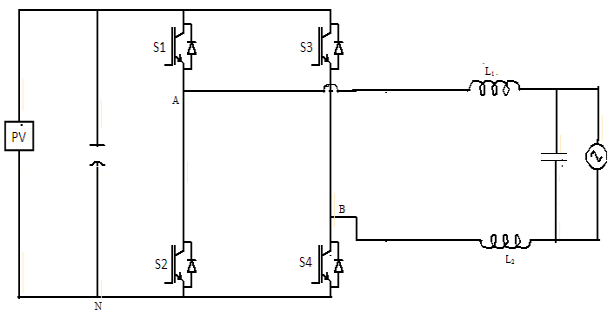

Fig. 5. H4 transformerless PV inverter.

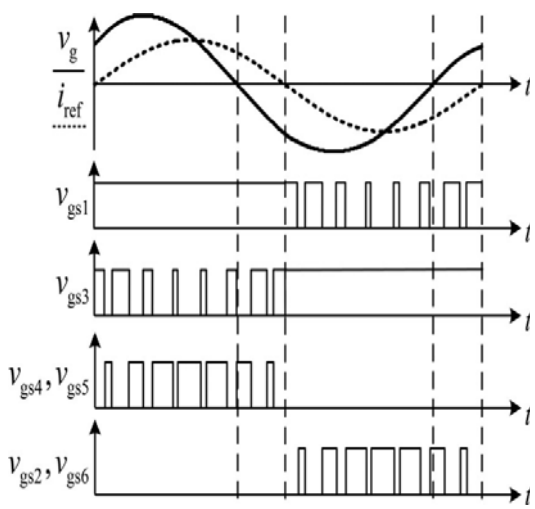

Fig. 6. Gate drive signals.

function of the modulating signal used in the sinusoidal pulse width modulation (SPWM).

III. Maximum Power Point Tracking

MPPT is the process of continuously harvesting the maximum available power that occasionally changes from time to time having a variable capability power source, such

as a PV power plant. The power generated from PV panels is a function of available solar irradiation. Therefore, with frequent changes in solar irradiation, the power that could be generated from PV panels varies accordingly. Under such conditions, if a fixed load is to be connected across a PV unit, the connected load for the PV unit could sometimes be underloaded or overloaded depending on the power being generated for the particular moment. On the basis of solar irradiation, the internal impedance of PV panels also changes. This condition leads to a serious challenge, that is, if the impedance of the connected load changes with the PV system from time to time, then deriving the maximum possible power from the PV unit becomes impossible. The process of altering the load side impedance from the PV unit according to the changes in such PV unit is actually the basis of MPPT.

In practice, should the load be of constant impedance, then a converter comes in between the load and the PV unit such that this converter precisely changes its input impedance to match the impedance between the PV unit and the input terminals of the converter. In this way, the converter can derive the maximum power from the PV unit and deliver it to the load in the required form.

The converter that comes in between the PV unit and the grid may be a DC to DC converter or a DC to AC converter depending upon the electrical load to be served. The function of the converter, in addition to changing power from the available form to the required form, is to ensure that the maximum derivable power for every moment is harvested from the PV unit.

In this research, we design a transformerless inverter system that comes in between the PV unit and the grid. The grid voltage requirement to be met by the inverter output is achieved only by connecting the required number of PV units in series so that the fundamental voltage is attained. The inverter is configured in the H6 format such that the common mode current is reduced. The control system, which is responsible for producing the required reference wave for generating the appropriate PWM, should ensure that the terminal voltage, frequency, and phase of the voltage at the output terminal of the inverter match those of the grid. Depending upon the variations in the solar irradiation, the power derivable from each PV unit changes along with the power delivered to the grid. These changes occur at constant voltage and frequency, but depending upon the power generated from the PV unit, the inverter-driven grid current changes. Irrespective of the quantum of the power delivered to the grid, this current should be sinusoidal and in phase with the voltage prevailing at the grid. To reduce the size of the passive filters, the PWM strategy is selected so that SPWM with a fairly high carrier frequency of 20 kHz is used, with the reference being coined according to requirements such as MPPT on the source side and power quality requirements on the grid side.

IV. Average Current Control Scheme

The simulation diagram of the control system is shown in Figure 7. If a certain power is to be delivered to the grid whose power and system voltage are known and if the power factor to be maintained in the power injection system is meant to be unity, then the current to be driven into the grid can be easily calculated. For example, if the power to be delivered to the grid is 300 W and if the RMS value of the voltage prevailing at the point of common coupling is 200 V RMS, then the value of the current is I = P/V such that I = 300/200 considering that the power factor = 1. Thus, the current is 1.5 A RMS or is a sinusoidal current wave of 50 Hz at the same phase as that of the voltage at the point of common coupling with the grid, and will have an amplitude of 1.414 × 1.5 A. This sinusoidal reference signal representing the required form of the current to be injected into the grid is compared against the current that is actually being injected into the grid. Thus, a continuous error signal is produced to be fed into a PI controller of a large bandwidth. As long as the solar insolation is constant, the current driven into the grid is assumed to be a sine wave of constant amplitude.

Whenever a change occurs in the solar insolation level, the MPPT unit sets a new reference power value to be harnessed; the current reference amplitude is altered accordingly (Figure 8).

A. Control Scheme

The product of V and I is the power being supplied by the PV panel at a certain moment. For this power to be pumped into the grid, the output voltage of the inverter must match the grid side voltage in terms of amplitude, phase, and frequency. Furthermore, the current entering the grid must be calculated according to the PV power available at the moment.

Power to be delivered into the grid = P
Grid side voltage Vg = 230 V RMS
Grid side frequency = fg = 50 Hz
Grid side phase = ϕg = 0 deg.

The values shown against the variables Vg, fg, and ϕg indicate the power estimated to be derived from the solar panel. This estimated power, as determined with the P&O algorithm, is used as the set power, and the current to be injected into the grid is found accordingly. The instantaneous value of the estimated current is constantly compared against the actual current, and the error is fed into the error detector and PI/FLC controller, which in turn generates the control quantity to be used in the PWM section.

B. Typical PI Controller

The PI controller integrates the error between the feedback and reference current to generate a variable voltage value. If a finite error exists for the moment, then the error is passed

TABLE I
FIS RULES

Error / Error rate	NB	NB	ZE	PS	PB
NB	NB	NB	NB	NS	ZE
NS	NB	NB	NS	ZE	PS
ZE	NB	NS	ZE	PS	PB
PS	NS	ZE	PS	PB	PB
PB	ZE	PS	PB	PB	PB

through the PI controller, and the output of the PI controller is used to alter the manipulated variable. With the possible negative feedback later, the error becomes zero. Although controllers with slowly varying controlled variables may feature low bandwidths, higher-bandwidth controllers for fast-varying controlled parameters are necessary. With the sinusoidal signal as reference, the controlled parameter exactly tracks the reference sinusoidal signal as in the case of the current mode controller used in the present work. After the estimation of the sinusoidal reference current for load, the actual load is compared, and the error is estimated. The error is fed to either the PI controller or the FLC. The performances of the PI controller and FLC are compared in this work. The Kp and Ki parameters are 0.01 and 0.02, respectively. The sampling rate used in the simulation is 10 μs.

C. Fuzzy Logic Controller

The same system is attempted for the FLC, and the Mamdani method for FLCs is used. The error, error rate, and output comprise five membership functions each. Table I shows 25 rules. The sliding rule-based inference scheme is employed. The editor window and sample input membership function editor window of error are shown in Figure 7. The surface view of the FLC is illustrated in Figure 9.

V. RESULTS AND DISCUSSION

The results obtained in the MATLAB/SIMULINK-based simulation and experimental verifications are discussed in this chapter.

A. Simulation in the MATLAB/SIMULINK Environment

Figure 5(a) shows the various sub systems of the simulation in the MATLAB/SIMULINK platform. Figure 14(c) illustrates the waveforms associated with the solar panel and presents the insolation, voltage output, and power output of the PV unit. Figure 15(c) reveals that the output power of the solar panel is a function of solar insolation. Thus, the P&O algorithm is evidently useful in harvesting maximum power. Figure 15(c) also demonstrates the efficiency of the H4 and H6 transformerless PV inverters at different insolation levels.

The core controller of the average current mode controller

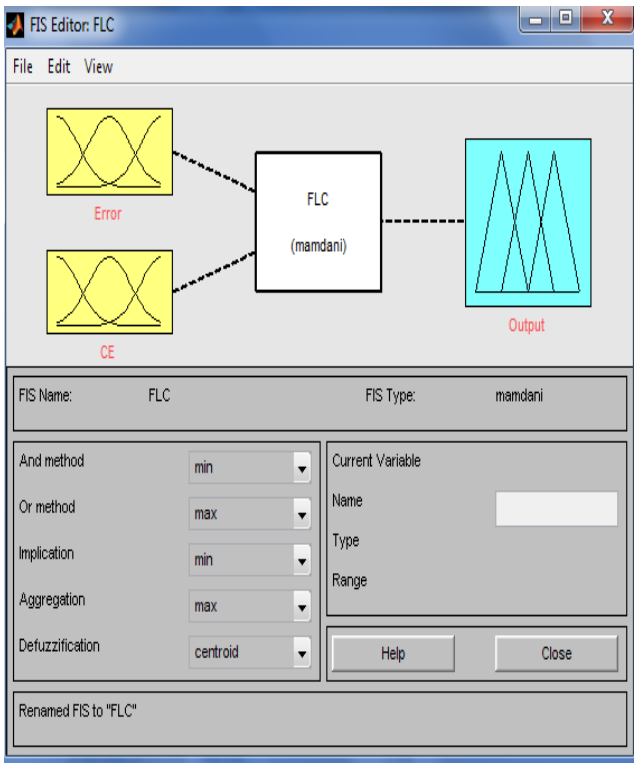

Fig. 7. Editor window of FLC.

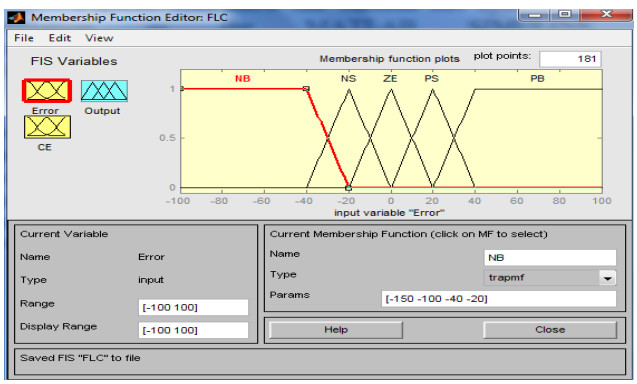

Fig. 8. Input membership function editor window – error.

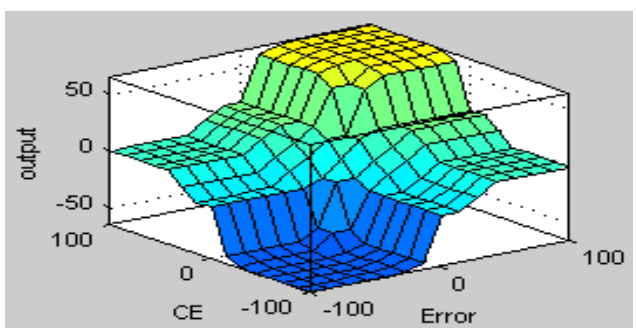

Fig. 9. Surface view of FLC.

can be either a PI controller or an FLC. In this research, both the PI controller and FLC are attempted. As shown in Figure 13(b), the FLC performs better than the PI controller in terms of the reduced THD to 1.34%.

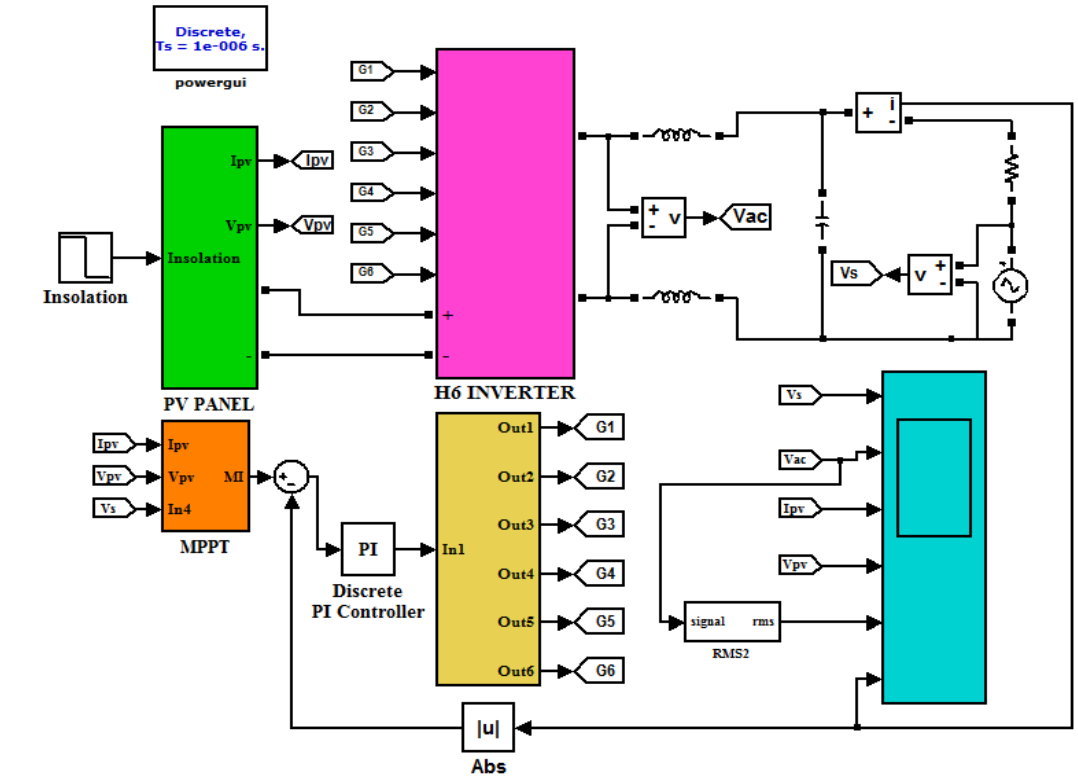

Fig. 10. SIMULINK model of H6 transformerless converter.

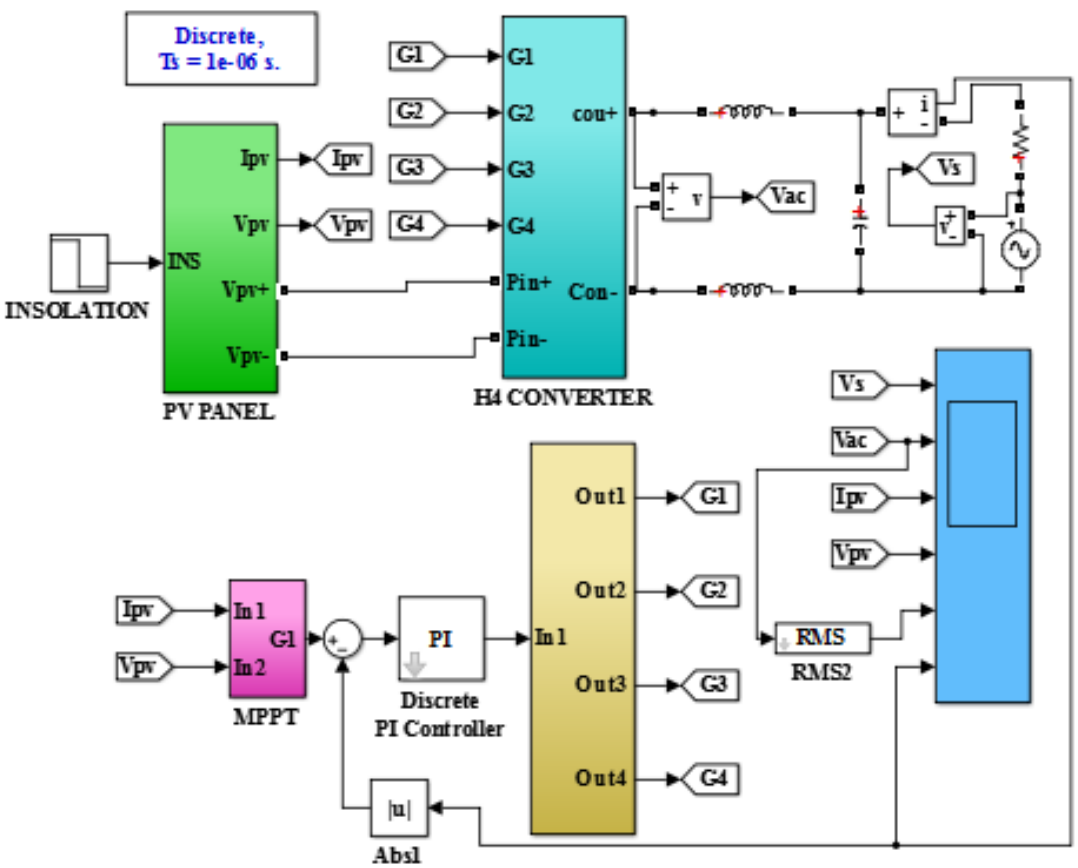

Fig. 11. SIMULINK model of H4 transformerless converter.

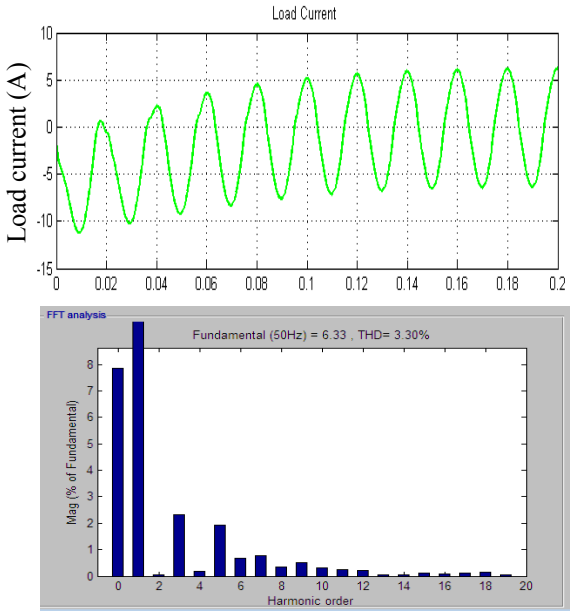

(a)

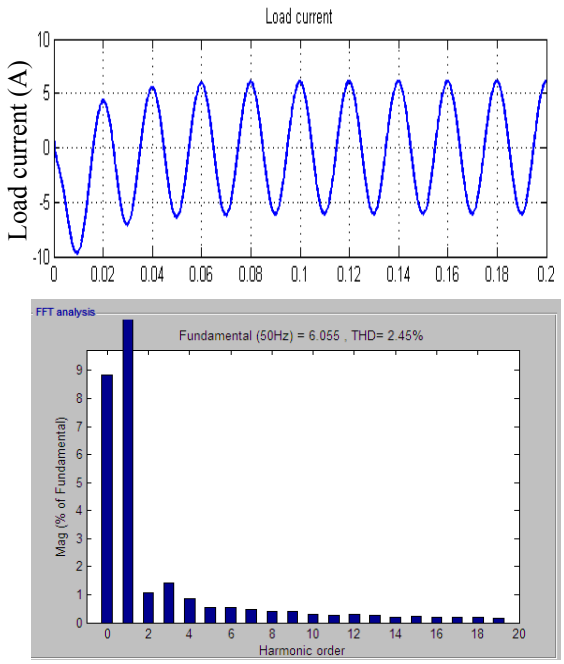

(b)

Fig. 12. H4 configuration. (a) Load current and THD for PI controller. (b) Load current and THD for FLC.

One of the objectives of the present work is to show that the H6 configuration is effective in mitigating the common mode leakage current. The common mode currents under the H4 and H6 versions of the inverter are recorded. As shown in Figures 14(a) and 14(b), the H6 configuration of the single-phase inverter offers a reduced common mode current.

Figures 16(a) and 16(b) show the pulses generated for driving the six switches of the H6 inverter and the four switches of the H4 inverter, respectively. The additional two sets of switching pulses are for the additional two switches of

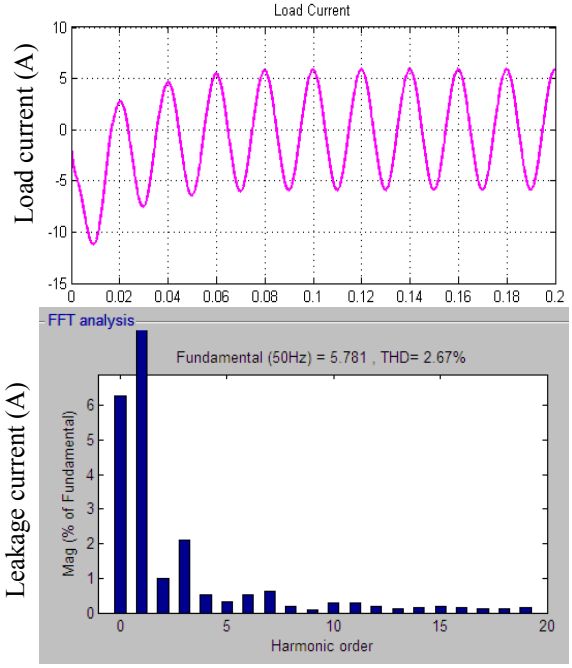

(a)

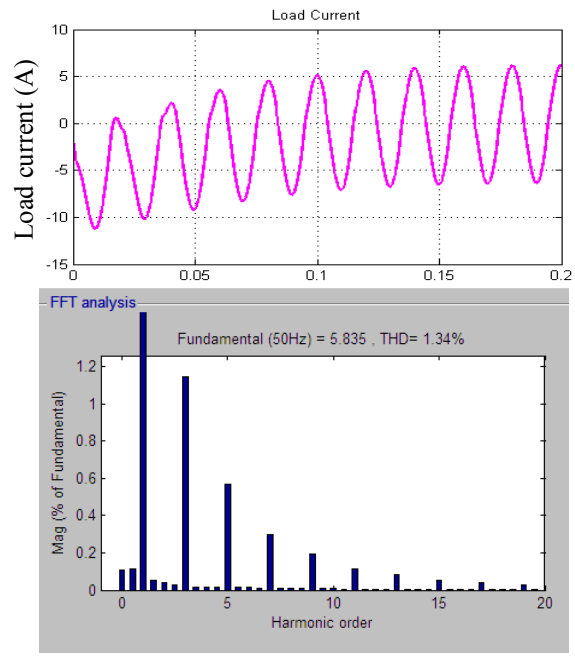

(b)

Fig. 13. H6 configuration. (a) Load current and THD for PI controller. (b) Load current and THD for FLC.

the H6 inverter. By appropriately disconnecting the solar panel from the grid, the common mode current is properly disrupted.

VI. Experimental Results

The specifications of the experimental unit with a solar panel and its specifications at an irradiance of 1,000 W/m2 and temperature of 25 °C are detailed below.

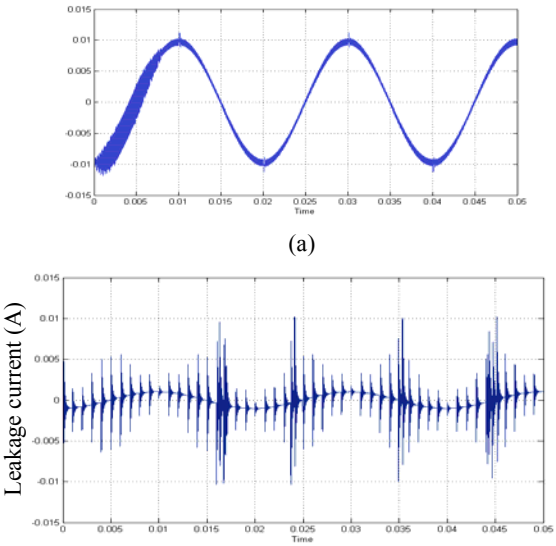

(a)

(b)

Fig. 14 (a) Common mode leakage current in H4 topology. (b) Common mode leakage current in H6 topology.

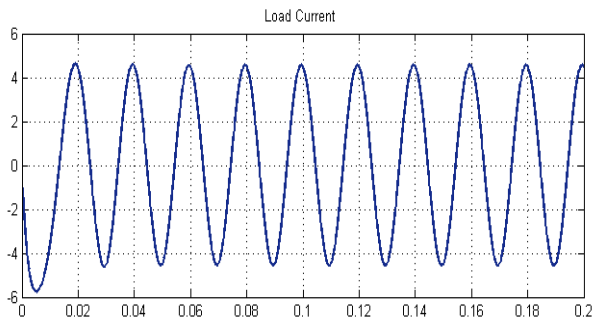

Fig. 15. Load current using the fuzzy controller with H6 configuration for disturbances in grid voltage.

Maximum power rating	220 W
Voc	22.2 × 20 = 444 v
Isc	.55 A
Vpmax/panel	17.5 v
Ipmax	.45A
Pmax	17.5 × 20 × 0.45 = 157.5 W
Central control system	PIC 16F 877A Processor
Optical isolation	MCT 2E ICs-6 Numbers

The values are nominal and may deviate slightly during real-time operation. To ensure a symmetric operation, the sample sine wave from the grid is derived and used by the controller. As for the control unit, the front-end controller section ensures that the output terminal voltage of the inverter is equal to that of the grid in terms of magnitude and frequency phase.

The second section of the controller drives the appropriate current into the grid. This current is a variable sinusoidal

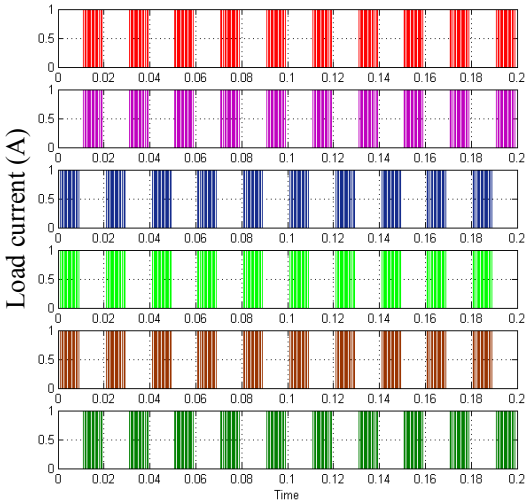

(a)

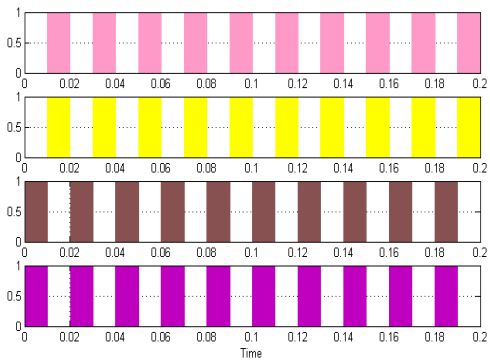

(b)

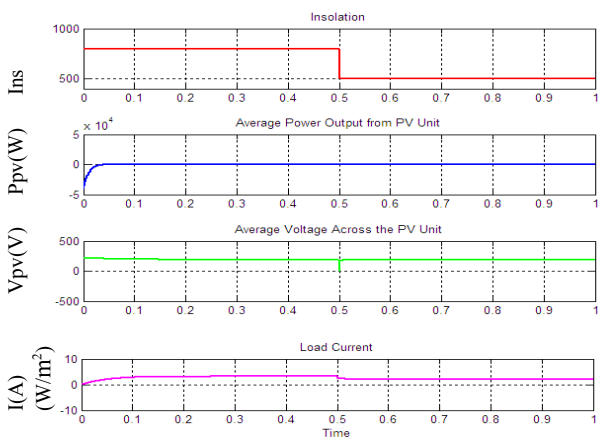

(c)

Fig. 16. (a) Gating pulses for H6 inverter. (b) Gating pulses for H4 inverter. (c) Waveforms associated with the solar panel.

current dictated by the MPPT scheme. The set point for the current is a function of the maximum power that can be derived from the PV unit at the given moment.

To satisfy the MPPT principle, the set current is given an increment periodically as a perturbation. If the power drawn from the PV unit rises, then the perturbation is continued in the same direction. By contrast, if a perturbation causes a

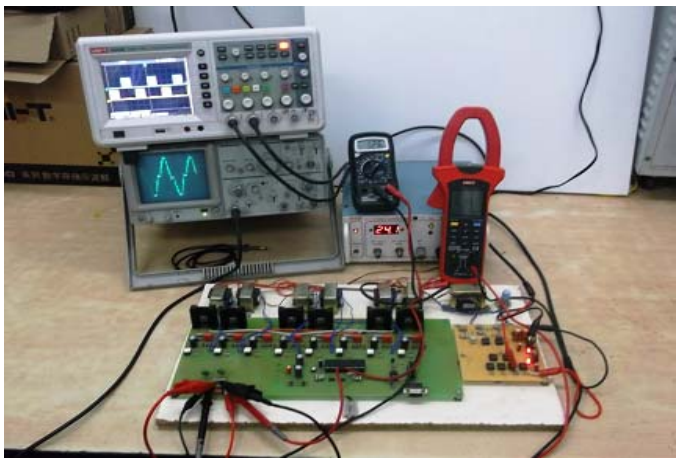

Fig. 17. Experimental setup.

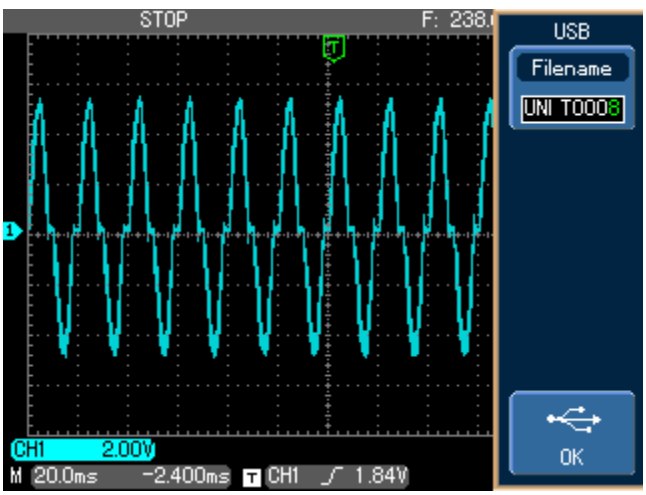

(a)

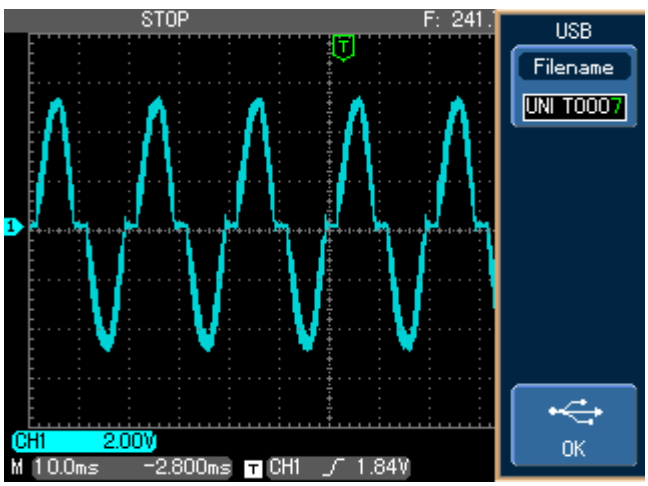

(b)

Fig. 18. Current injected into the grid. (a) PI controller. (b) FLC.

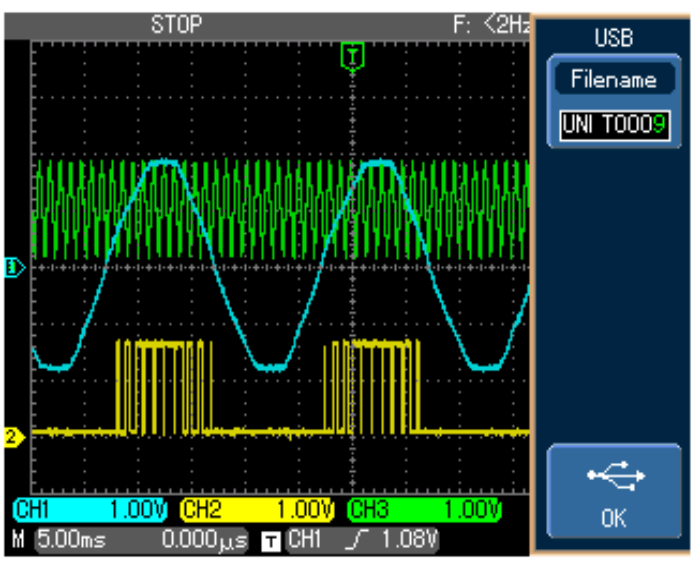

(a)

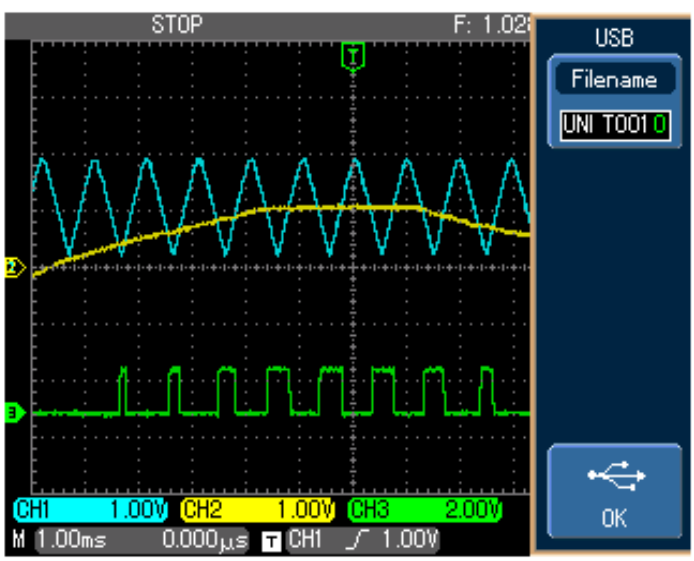

(b)

Fig. 19. Experimental gate pulses.

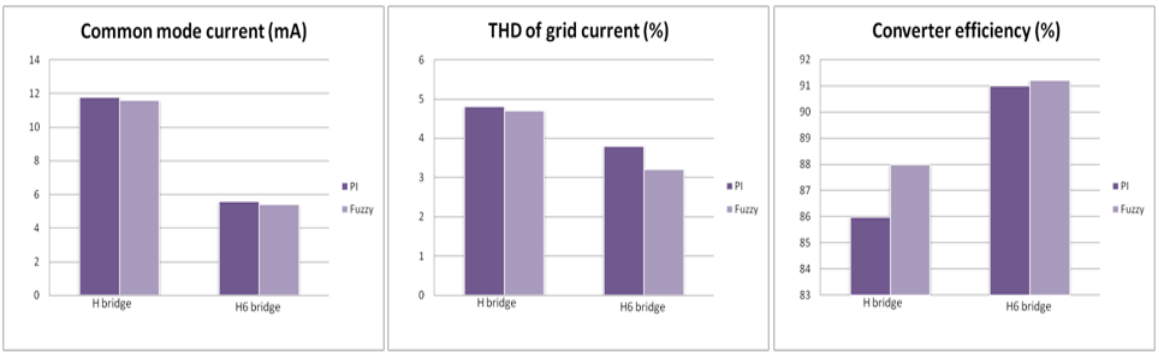

(a)

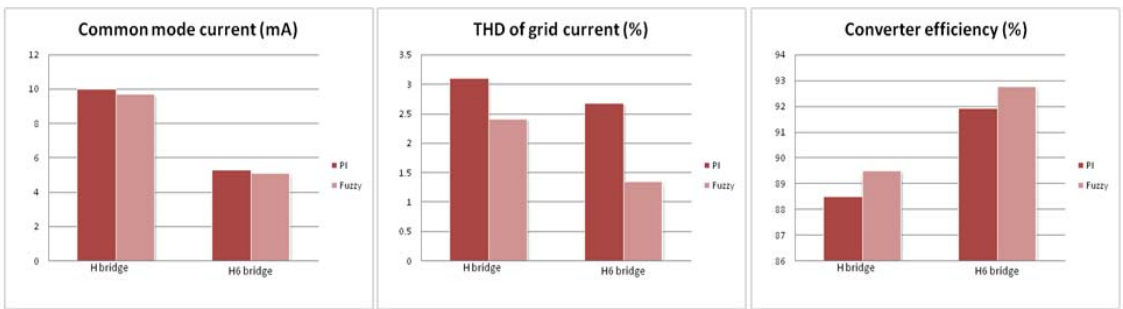

(b)

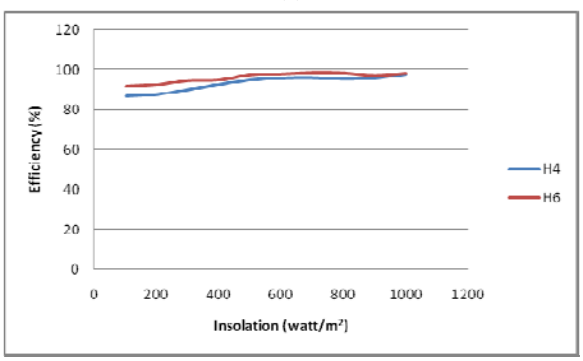

(c)

Fig. 20. Graphical comparison of the performances of the H4 and H6 bridges. (a) Experimental results. (b) Simulation results. (c) Efficiency of H4 and H6 inverters under different insolations.

reduction in power output, then the perturbation is continued in the reverse direction.

A. Details of the Experimental Setup

The experimental setup to validate the proposed idea is carried out with a capacity to handle and deliver a nominal power of 80 W into the 230 V 50 Hz utility point. Considering the maximum power rating of 157.5 W (17.5 × .45 × 20), we use a set of 20 PV panels in series connection.

The master control unit is centered around the PIC micro-controller 16F877A. Isolated power supplies are used by the MCT2E optocouplers to bring the switching signals to the MOSFETs. The MOSFETs are of the IRF840 type with 500 V and 8 A. With the maximum voltage of 345 V across the PV system and 20 panels in series, the maximum possible peak voltage of the fundamental is

$$\begin{aligned} V_{peakfund} &= 4 \times V_{dc}/Pi \\ &= 4 \times 345/3.14 \\ &= 439\ V \\ V_{RMS} &= 439/1.414 = 311\ V \end{aligned}$$

By controlling the modulation index, this voltage can be controlled linearly down to zero. The approximate value of the modulation index for an RMS voltage of 230 V is 230/311 = 0.7395. The RMS value of the current entering the grid while delivering the maximum power of 157 W is 157/230 = 0.6847 A.

Figure 17 presents the waveform of the AC current injected into the grid while Figure 18 illustrates the waveforms related to the sinusoidal PWM. The triangular carrier and modulating signal are compared in a set of two

TABLE I
COMPARISON OF H4 BRIDGE AND H6 BRIDGE

Parameters	Simulation results				Experimental results			
	H4 bridge		H6 bridge		H4 bridge		H6 bridge	
	PI	Fuzzy	PI	Fuzzy	PI	Fuzzy	PI	Fuzzy
Common mode current	10 mA	9.7 mA	5.3 mA	5.1 mA	11.8 mA	11.6 mA	5.6 mA	5.4 mA
THD of grid current	3.3%	2.45%	2.67%	1.34%	4.8%	4.7%	3.8%	3.2%
Converter efficiency	88.5%	89.5%	91.9%	92.75%	86%	88%	91%	91.2%
Integral square error (ISE)	234	198	123	110	254	205	149	120
Tracking period	36 μs	24 μs	34 μs	25 μs	39 μs	28 μs	38 μs	28 μs

channels of the DSO. A zoomed view of the PWM pulses is also shown for the sake of clarity.

Table I presents the results of the experimental verification. The same arguments in terms of the comparison of the H4 and H6 configurations with the PI and FLC control schemes apply in the practical scenario of experimental verification. However, some deviations can be observed in all the three performance parameters considered for the simulation and experimental verification.

Table I compares the performance parameters of the H4 and H6 inverter units. The H4 and H6 cases in which the PI controllers are applied reveal that the H6 configuration offers a peak value of leakage current of only 5.3 mA, which is lower than the 10 mA leakage current of the H4 inverter case.

According to Table I, the performances of the FLC under the H4 and H6 configurations are also compared. The fuzzy logic scheme of control notably performs satisfactorily in terms of the reduced leakage current, which is 5.1 mA in the case of the H6 inverter and 9.7 mA in the case of the fuzzy logic-controlled H4 inverter.

The THD of the current fed into the grid is as low as 1.34% in the case of the FLC-controlled H6 configuration and as high as 2.6% in the case of the PI- controlled H6 configuration. The H4 configuration of the single-phase inverter is found to involve high THDs of 3.3% and 2.45% for the PI and FLC schemes, respectively.

By contrast, the efficiency of the power conversion system with the H6 configuration is higher than that of the power conversion system with the H4 configuration. Under both control schemes viz. PI and FLC, the efficiencies of the H6 inverter configuration are 91.9% and 92.75%, respectively, which are higher than those of the H4 inverter scheme with the PI and FLC strategies (i.e., 88.5% and 89.5%, respectively). The aforementioned results relate to the simulations in the MATLAB/SIMULINK environment. The experimental verifications also validate the simulations, as shown in the following discussions.

Tolerances in the test and measuring instruments could play a major role in the deviations of the results of the experimental verification. Voltage drop in semiconductor devices and the effects of temperature also influence the results.

However, the deviations observed between the simulation and the experimental verifications do not influence a sensible comparison between the proposed idea, that is, using the H6 inverter with an average current control mode with fuzzy logic and PI control schemes, and the application of the same control techniques with the H4 inverter scheme.

Therefore, we can conclude that the FLC strategy with the H6 inverter topology for implementing the average current control mode of power injected into the grid from a PV unit with the P&O algorithm is feasible and effective.

VII. CONCLUSION

This study proposes an H6 inverter with MPPT. In addition to the P&O-based MPPT technique, the average current mode control technique for injecting sinusoidal source currents into the grid has also been attempted / applied to the control system. The P&O algorithm captures the maximum power point, and the average current mode control ensures that the sinusoidal current is injected into the grid. Two control schemes, namely, PI control scheme and FLC scheme, are developed. These controllers are implemented and studied alternately on the current injection side of the grid. The observations on the simulations and the experimental verifications reveal that the H6 inverter offers a reduced leakage current in comparison with the H4 inverter. In this application of injecting power into the grid by using the H6 converter, the FLC outperforms the PI-based controller in terms of injected power quality. The FLC can be concluded to outperform PI in terms of efficiency improvement from 88% to 91.2%. Similarly, FLC causes the THD to decrease by 1.5% from 4.7% to 3.2%. Multi-level inverters with harmonic reduction techniques, such as selective harmonic elimination and space vector PWM, can also be attempted in this application. Such multi-level inverters are recommended. The outcome of this study widens the research scope for a single comprehensive control system to ensure maximum power harvesting while ensuring power quality.

REFERENCES

[1] D. J. Arent, A. Wise1, and R. Gelman, "The status and prospects of renewable energy for combating global warming", *Elseiver Energy Economics*, Vol. 33, No. 4, pp. 584-593, Jul. 2011

[2] F. Blaabjerg, Z. Chen, and S. B. Kjaer, "Power electronics as efficient interface in dispersed power generation systems," *IEEE Trans. Power Electron.*, Vol. 19, No. 5, pp. 1184-1194, Sep. 2014.

[3] L. Zhang, K. Sun, Y. Xing, and M. Xing, "H6 transformerless full-bridge PV grid-tied inverters," *IEEE Trans. Power Electron.*, Vol. 29, No. 3, pp. 1229-1238, Mar. 2014.

[4] W. Yu, J.-S. Lai, H. Qian, C. Hutchens, J. Zhang, G. Lisi, A. Djabbari, G. Smith, and T. Hegarty, "High-efficiency MOSFET inverter with H6-type configuration for photovoltaic nonisolated AC-module applications," *IEEE Trans. Power Electron.*, Vol. 26, No. 4, pp. 1253-1260, Apr. 2011.

[5] B. Ji, J. Wang, and J. Zhao, "High-efficiency single-phase transformerless PV H6 inverter with hybrid modulation method," *IEEE Trans. Ind. Electron.*, Vol. 60, No. 5, pp. 2104 -2115, Oct. 2012.

[6] R. Gonzalez, E. Gubia, J. Lopez, and L. Marroyo, "Transformerless single-phase multilevel-based photovoltaic inverter," *IEEE Trans. Ind. Electron.*, Vol. 55, No. 7, pp. 2694-2702, Jul. 2008.

[7] H. Patel and V. Agarwal, "A single-stage single-phase transformer-less doubly grounded grid-connected PV interface," *IEEE Trans. Energy Convers.*, Vol. 24, No. 1, pp. 93-101, Feb. 2009.

[8] S. Aeaujo, P. Zacharias, and R. Mallwitz, "Highly efficient single-phase transformerless inverters for grid-connected photovoltaic systems," *IEEE Trans. Ind. Electron.,* Vol. 57, No. 9, pp. 3118-3128, Aug. 2010.

[9] H. Xiao and S. Xie, "Transformerless split-inductor neutral point clamped three-level PV grid-connected inverter," *IEEE Trans. Power Electron.,* Vol. 27, No. 4, pp. 1799-1808, Feb. 2012.

[10] M. C. Cavalcanti, K. C. de Oliveira, A. M. de Farias, F. A. S. Neves, G. M. S. Azevedo, and F. C. Camboim, "Modulation techniques to eliminate leakage currents in transformerless three-phase photovoltaic systems," *IEEE Trans. Ind. Electron.*, Vol. 57, No. 4, pp. 1360-1368, Mar. 2010.

[11] O. Lopez, F. D. Freijedo, A. G. Yepes, F. Comesana, J. Malvar, R. Teodorescu, and J. Doval-Gandoy, "Eliminating ground current in a transformerless photovoltaic application," *IEEE Trans. Energy Convers.*, Vol. 25, No. 1, pp. 140-147, Mar. 2010.

[12] H. Xiao and S. Xie, "Leakage current analytical model and application in single-phase transformerless photovoltaic grid-connected inverter," *IEEE Trans. Electromagnetic Compat.,* Vol. 52, No. 4, pp. 902-913, Nov. 2010.

[13] B. Yang, W. Li, Y. Gu, W. Cui, and X. He, "Improved transformerless inverter with common-mode leakage current elimination for a photovoltaic grid-connected power system," *IEEE Trans. Power Electron.,* Vol. 27, No. 2, pp. 752-762, Feb. 2012.

[14] M. A. G. de Brito, L. Galotto, and L. P. Sampaio, "Evaluation of the main MPPT techniques for photovoltaic applications," *IEEE Trans. Ind. Electron.,* Vol. 60, No. 3, pp. 1156-1167, Mar. 2013.

[15] A. R. Reisi, M. H. Moradi, and S. Jamasb, "Classification and comparison of maximum power point tracking techniques for photovoltaic system: A review," *Elseiver, Renewable and Sustainable Energy Reviews*, Vol. 19, pp.433-443, Mar. 2013.

[16] N. Femia, G. Petrone, G. Spagnuolo, and M. Vitelli, "Optimization of perturb and observe maximum power point tracking method," *IEEE Trans. Power Electron.,* Vol. 20, No. 4, pp. 963-973, Jul. 2005.

[17] S. K. Kollimalla, and M. K. Mishra, "A novel adaptive P&O MPPT algorithm considering sudden changes in the irradiance," *IEEE Trans. Energy Convers.,* Vol. 29, No. 3, pp. 602-610, Sep. 2014.

[18] X. Gao, S. Li, and R. Gong, "Maximum power point tracking control strategies with variable weather parameters for photovoltaic generation systems," *Elseiver, Solar Energy,* Vol. 93, pp. 357-367, Jul. 2013.

[19] J. A. S. Morales, J. Leyva-Ramos, E. E. G. Carbajal, and M. G. Ortiz-Lopez, "Average current-mode control scheme for a quadratic buck converter with a single switch," *IEEE Trans. Power Electron.,* Vol. 23 , No.1 , pp. 485-490, Jan. 2008 .

[20] Y. Yan, F. C. Lee, P. Mattavelli, and P.-H. Liu, "Average current mode control for switching converters," *IEEE Trans. Power Electron.,* Vol. 29, No. 4, pp. 2027-2036, Apr. 2014.

A. Radhika was born in Sivagangai, in 1980. She received her B.E. (EEE) degree from Madurai Kamaraj University, Madurai, Tamilnadu, India, and her M.E. (PED) degree from Anna University, Tirunelveli, Tamilnadu, India, in 2003 and 2009, respectively. She is currently working toward her Ph.D. in Electrical Engineering from Anna University, Chennai, Tamilnadu, India. From 2004 to 2007, she was an Assistant Professor in various Engineering colleges, such as the Raja College of Engineering and Technology and the Pandiyan Saraswathi Yadava College of Engineering and Technology. Since 2011, she has been an Assistant Professor of Electrical and Electronics Engineering in the Velammal College of Engineering & Technology, Madurai, Tamilnadu, India. Her research area covers the augmentation of various inverters for the mitigation of harmonics and reduction of common mode leakage currents with renewable energy systems

A. Shunmugalatha was born in Virudhunagar, in 1969. She received her B.E. (EEE) and M.E. (PSE) degrees from Madurai Kamaraj University, Madurai, Tamilnadu, India, in 1990 and 2000, respectively, and her Ph.D. degree in Electrical Engineering from Anna University, Chennai, Tamilnadu, India, in 2009. From 1992 to 2010, she was an Assistant Professor in various Engineering colleges, such as the Dr. MGR Engineering College and K.L.N College of Engineering. Since 2010, she has been a Professor and Head of Electrical and Electronics Engineering in Velammal College of Engineering & Technology, Madurai, Tamilnadu, India. Her research area covers power system stability studies using optimization techniques.